

Mass varying neutrinos in supernovaeF. Rossi-Torres,^{1,2,*} M. M. Guzzo,^{1,†} P. C. de Holanda,^{1,‡} and O. L. G. Peres^{1,3,§}¹*Instituto de Física Gleb Wataghin-UNICAMP, 13083-859, Campinas SP, Brazil*²*Instituto de Física Teórica, Universidade Estadual Paulista, Rua Dr. Bento Teobaldo Ferraz, 271-BI. II, 01140-070, São Paulo, SP, Brazil*³*The Abdus Salam International Centre for Theoretical Physics, I-34100 Trieste, Italy*

(Received 13 January 2011; published 21 September 2011)

We study the consequences on the neutrino oscillation parameter space, mixing angle ($\tan^2\theta$), and vacuum mass difference (Δm_0^2) when mass varying neutrino (MaVaN) models are assumed in a supernova environment. We consider electronic to sterile channels $\nu_e \rightarrow \nu_s$ and $\bar{\nu}_e \rightarrow \bar{\nu}_s$ in two-flavor scenario. In a given model of MaVaN mechanism, we induce a position-dependent effective mass difference, $\Delta\tilde{m}^2(r)$, where r is the distance from the supernova core, that changes the neutrino and antineutrino flavor conversion probabilities. We study the constraints on the mixing angle and vacuum mass difference coming from r-process and the SN1987A data. Our result is the appearance of a new exclusion region for very small mixing angles, $\tan^2\theta = 10^{-6}$ – 10^{-2} , and small vacuum mass difference, $\Delta m_0^2 = 1$ – 20 eV², due the MaVaN mechanism.

DOI: [10.1103/PhysRevD.84.053010](https://doi.org/10.1103/PhysRevD.84.053010)

PACS numbers: 13.15.+g, 14.60.Pq, 14.60.St

I. INTRODUCTION

Evidences from experimental data of type Ia supernovae (SNIa) [1,2], cosmic microwave background (CMB) radiation [3], and large scale structure (LSS) [4] point out that our universe is in accelerated expansion. One possible explanation for this acceleration is dark energy which contains 70% of the total energy of our universe. Dark energy could be a cosmological constant (Λ), or simply, the nonzero vacuum energy, which is quite close to the critical cosmological energy density, $\rho_c \approx \rho_\Lambda \approx 4 \times 10^{-47}$ GeV⁴. However one critical point of Λ is the necessity of a fine tuning, once that according to theoretical expectations, ρ_{vac} is 10^{50} – 10^{120} larger than the magnitude allowed in cosmology. In Ref. [5], Dolgov emphasizes

- (1) *Why vacuum energy, which must stay constant in the course of cosmological evolution, or dark energy, which should evolve with time quite differently from the normal matter, have similar magnitude just today, all being close to the value of the critical energy density?*
- (2) *If universe acceleration is induced by something which is different from vacuum energy, then what kind of field or object creates the observed cosmological behavior? Or could it be a modification of gravitational interactions at cosmologically large distances?*

From the questions above, other candidates for dark energy have been proposed, such as: quintessence,

K-essence, tachyon field, phantom field, dilatonic dark energy, Chaplygin gas (for excellent reviews see [6]).¹

Furthermore, neutrinos are powerful tools for astronomy investigation [7], and they play a crucial role in the mechanism of supernova explosion, according to the standard scenario [8]. Based on the very interesting fact that the scale of the neutrino squared mass difference ($(0.01 \text{ eV})^2$) is similar to the dark energy scale, the possibility of neutrino coupling with a scalar field naturally arises. Hung [9] developed the idea that sterile neutrinos could have a relation with the accelerating universe. He proposed that the sterile neutrino obtains its mass through a Yukawa coupling with a singlet scalar field whose effective potential is of a “slow-rolling” type in which the vacuum energy is given approximately by ρ_{vac} and the effective mass of the sterile neutrino is proportional to the expectation value of the scalar field. When this scalar field evolves, the sterile neutrino mass changes. Fardon *et al.* describe that the total energy of the cosmological fluid can vary slowly as the neutrino density decreases [10], in a similar way of Hung’s model. Consequently, the coupling with a scalar field causes a variation of the neutrino mass (dynamical field) proportional to the local neutrino density and perhaps to the baryonic matter [11]. This picture has been called Mass Varying Neutrino (MaVaN) models. Afshordi *et al.* [12] and Bjalde *et al.* [13] showed that the proposed MaVaN models, in the nonrelativistic regime, could be threatened by the strong growth of hydrodynamic perturbations associated with a negative adiabatic squared sound speed.

*ftorres@ift.unesp.br

†guzzo@ifi.unicamp.br

‡holanda@ifi.unicamp.br

§orlando@ifi.unicamp.br

¹There are alternative scenarios to explain the acceleration, such as modified gravity with an introduction of quantum effects—higher curvature corrections—to the Einstein-Hilbert action.

Many articles have treated neutrino oscillation via the MaVaN mechanism [14–22]. We observe, nevertheless, that these articles focus on solar and atmospheric neutrinos, as well as observations from accelerators and reactors. However, the assumption of MaVaN mechanism in the neutrino evolution in supernovae environments has not been fully explored yet. In fact, the only article that connects MaVaN and supernova is Li *et al.* [23], which use data from a type Ia supernova to limit the interactions between neutrinos and scalar dark energy.

In this paper, therefore, we investigate the consequences of MaVaN mechanisms on the neutrino propagation in a supernova environment. We take into consideration that recent results from WMAP-7 [24] indicate that the number of species of relativistic neutrinos is equal to 4.34 ± 0.87 which, in contrast with the standard model three active neutrinos, suggest that there may be additional species of neutrinos, for example, a sterile one ν_s , possibly an SU(2) singlet. These sterile neutrinos can present masses ranging from a few eV to values larger than the electroweak scale [25]. Therefore, a natural and potentially interesting investigation can arise from the analyses of (anti) neutrino oscillations $\nu_e \rightarrow \nu_s$ and $\bar{\nu}_e \rightarrow \bar{\nu}_s$ in supernovae under the assumption that MaVaN models are implemented. We evaluate the consequences of such (anti)neutrino oscillations on the signal of $\bar{\nu}_e$ and ν_e in terrestrial detectors, as well as on supernova heavy-element nucleosynthesis (r-process).

The crucial point of our analysis is the fact that MaVaN model can directly affect the relevant parameter for neutrino oscillations, namely, the squared mass difference, Δm_0^2 . We propose a phenomenological MaVaN model that is more convenient to test using neutrinos from supernova. Such parameterization allows to fit the amplitude of the Δm_0^2 variation, the position where the variation begins, and also if the masses will increase or decrease along the neutrino trajectory. We use this parameterization to evaluate the constraints on the oscillation parameter space, $\tan^2\theta \times \Delta m_0^2$ (where θ and Δm_0^2 are the mixing angle and the squared mass difference in vacuum, respectively), coming from the r-process nucleosynthesis condition, $Y_e < 0.5$ [26,27], and by the limit for the average survival probability coming from SN1987A data, $\langle P \rangle < 0.5$. Note that problems and criticisms to these MaVaN models were pointed by Peccei in Ref. [28].

The conclusion of our analysis is the following. With our MaVaN parameterization, significant modifications happen in the probability isocurves in (anti)neutrino parameter space, leading to new regions of exclusion. This happens particularly when the evolution of mass-squared difference inside the star is sufficiently slow to avoid nonadiabatic conversions. Besides, we find that the r-process nucleosynthesis is not affected by the MaVaN assumption.

This article is organized as follows: Section II presents the neutrino oscillation mechanism and the assumptions

and approximations used in our work. Section III presents our proposition of a new parameterization of MaVaN model. Section IV contains our results and related discussion. Finally Sec. V summarizes our conclusions.

II. NEUTRINO OSCILLATION AND SUPERNOVA NEUTRINO SPECTRUM

Supernova flavor spectra are not known with precision. In fact, several degeneracies are presented in neutrino emission parameters, as it is shown in [29]. Therefore, we will focus on an unpretentious approach: how the pattern of flavor conversion is affected by the inclusion of MaVaN in a supernova environment. In this framework, we assume a two-neutrino oscillation phenomenon and that some typical emission spectrum can be representative of a wide range of possibilities. Although this is a very naive approach, it is sufficient to appreciate the general features of the important modifications in the neutrino oscillation pattern introduced by MaVaN in a supernova environment.

Some comments about the assumptions for the neutrino oscillations we are interested in this article are in order. From the neutrino phenomenology we know the existence of two small mass scales, Δm_{atm}^2 and Δm_{sun}^2 , and two large mixing angles, θ_{21} and θ_{23} , and one small angle, if not vanishing, θ_{13} . We are interested in oscillations between active electronic into sterile neutrinos as well as oscillations between active electronic into sterile antineutrinos in a supernova environment. For this purpose we will include a new scale, Δm_0^2 . This new scale needs to be much larger than the small scales for active neutrinos— $\Delta m_0^2 \gg \Delta m_{\text{atm},\text{sun}}^2$ —in order to be compatible with constraints for sterile neutrinos.²

Such oscillations must be treated considering that both neutrino and antineutrino conversion can be resonantly enhanced in matter, the so-called Mikheyev-Smirnov-Wolfenstein (MSW) phenomenon [31]. Nevertheless, for a convenient choice of the squared mass difference in vacuum, we are allowed to neglect the conversion to sterile neutrinos in the inner core, for all values of the mixing angles we considered [32]. We will assume therefore that $1 \text{ eV}^2 < \Delta m_0^2 < 10^4 \text{ eV}^2$, always positive. Consequently, neutrinos carrying tens of MeV of energy will not suffer any resonance, since the core matter density is approximately 10^{14} g/cm^3 . Then the electronic potential is so high that no resonance will occur for any mixing angle inside the core. Furthermore, one neglects $\nu - \nu$ forward-scattering contribution to the weak potentials in first approximation after neutrinos have escaped from the inner core of the star. Recently, issues of self neutrino interactions were discussed considering three families by Dasgupta [33] and Friedland [34]. An analysis of self

²For an analysis of sterile neutrino oscillations in cosmological, astrophysical, and terrestrial media with various mixing and a wider range of Δm_0^2 see [30].

neutrino interactions considering two families was done in [35,36].

The equation which governs the flavor neutrino eigenstates evolution along their trajectory inside the supernova can be written as

$$i \frac{\partial}{\partial r} \begin{bmatrix} \Psi_e(r) \\ \Psi_s(r) \end{bmatrix} = \begin{bmatrix} \phi_e(r) & \sqrt{\sigma} \\ \sqrt{\sigma} & -\phi_e(r) \end{bmatrix} \begin{bmatrix} \Psi_e(r) \\ \Psi_s(r) \end{bmatrix}, \quad (1)$$

where

$$\phi_e(r) = \frac{1}{4E} (\pm 2V(r)E - \Delta m_0^2 \cos 2\theta), \quad (2)$$

and

$$\sqrt{\sigma} = \frac{\Delta m_0^2}{4E} \sin 2\theta, \quad (3)$$

with $\Delta m_0^2 > 0$. Under the assumptions described above, the matter potential can be written as follows:

$$V(r) = \sqrt{2}G_F \left[N_{e^-}(r) - N_{e^+}(r) - \frac{N_n(r)}{2} \right]. \quad (4)$$

In Eq. (2), the signal + is for neutrino, whereas the - signal is for antineutrinos. Δm_0^2 is the squared mass difference between two neutrinos mass eigenstates in vacuum; G_F is the Fermi coupling constant; θ is the vacuum mixing angle; and $N_{e^-}(r)$, $N_{e^+}(r)$, and $N_n(r)$ are, respectively, the number densities of electrons, positrons, and neutrons. $N_p = N_{e^-} - N_{e^+}$, which is the number density of protons, does not appear in Eq. (4) because electric charge neutrality of the medium was assumed. Note that neutrinos (antineutrinos) undergo in a resonance when

$$V(r) = \pm \frac{\Delta m_0^2}{2E} \cos 2\theta. \quad (5)$$

The range for θ parameter is $0 \leq \theta \leq \pi/2$. Our results can also be extended for the neutrino case oscillation, where the results in the region of $0 \leq \theta \leq \pi/4$ for antineutrinos will be the same for the neutrinos in the region of $\pi/4 \leq \theta \leq \pi/2$ and vice-versa.

The matter potential can be rewritten as

$$V(r) = \frac{3G_F \rho(r)}{\sqrt{2}m_N} \left(Y_e - \frac{1}{3} \right), \quad (6)$$

where Y_e is the electronic fraction

$$Y_e(r) = \frac{N_{e^-}(r) - N_{e^+}(r)}{N_p(r) + N_n(r)}, \quad (7)$$

m_N is the nucleon mass, and $\rho(r)$ is the matter density profile.

We will consider that the spectrum of neutrino emission can be written as [37]

$$\frac{dN}{dE} = \frac{L}{F(\eta)T^4} \frac{E^2}{e^{E/T-\eta} + 1}, \quad (8)$$

where η is the pinching factor and $F(\eta) = \int_0^\infty dx x^3 / (e^{x-\eta} + 1)$. For this spectrum $\langle E \rangle / T \approx 3.1514 + 0.1250\eta + 0.0429\eta^2 + O(\eta^3)$. Typical values of η are $\eta_{\nu_e} \sim 2$, $\eta_{\bar{\nu}_e} \sim 3$, and $\eta_x \sim 1$ [38]. The average energy of neutrino species is $\langle E_{\nu_e} \rangle \approx 11$ MeV, $\langle E_{\bar{\nu}_e} \rangle \approx 16$ MeV, $\langle E_{\nu_x} \rangle \approx 25$ MeV ($x = \mu, \tau$). L is the neutrino luminosity, which is approximately 10^{51} erg s⁻¹, and it can be considered equal for all neutrino flavors. Other choice of parameter spectra in Eq. (8), using codes such as those ones presented in [39,40], can be extracted. We use in this work the electronic potential profile for a supernova with a post bounce time evolution equal to $t_{pb} = 2s$, where the size of the neutrinosphere is approximately equal to the core size and the supernova is in the stage where heavy nuclei start to form.

In the MSW effect, the computation of the neutrino probabilities can have two regimes, the adiabatic regime which depends only on mixings of neutrinos in the initial and final point (and then can be calculated analytically) or the nonadiabatic regime, which depends on the path crossed by the neutrinos and can be found by solving numerically the Eq. (1). In standard scenario, all adiabatic effects for small mixings happen for $\Delta m_0^2 \gtrsim 100$ eV². For the results shown here, we will use the averaged probability over the neutrino spectrum described in Eq. (8).

III. MASS VARYING NEUTRINO MODEL

We adopt a phenomenological approach in modeling the MaVaN mechanism.³ We will implement the MaVaN mechanism by changing the mass-squared difference in vacuum (Δm_0^2) to a mass-squared difference ($\Delta \tilde{m}^2$) that depends on the neutrino density (n_ν) of the environment. In principle, we can also change the mixing angle, but we prefer to avoid this for simplicity. Also, the squared mass difference in MaVaN framework is the same for neutrinos and antineutrinos, $(\Delta \tilde{m}^2)_\nu = (\Delta \tilde{m}^2)_{\bar{\nu}}$.

We choose a parameterization for squared mass difference ($\Delta \tilde{m}^2$) in the MaVaN scenario such that we have, *at same time*, MaVaN induced effects and MSW effects [31]. For this we build the following function

$$\Delta \tilde{m}^2(r) = \Delta m_0^2 - \frac{\delta}{1 + (n_\nu(r)/n_\nu^0)^{-\eta}}, \quad (9)$$

where the neutrino density, $n_\nu(r)$, assuming that the neutrinos are equally produced in the neutrinosphere with radius $R_\nu \sim 10$ km, is given by

$$n_\nu(r) = \frac{L}{\langle E_\nu \rangle} \frac{1}{8\pi c R_\nu r} \ln \left(\frac{r + R_\nu}{r - R_\nu} \right), \quad (10)$$

where r is the radial distance measured from R_ν and c the speed of light. For larger radius $r \gg R_\nu$, the neutrino

³In [41] it was proposed a phenomenological construction of a MaVaN model in the cosmological context.

density is written as $n_\nu \sim r^{-2}$. The parameters n_ν^0 and η are constants to be chosen. For $n_\nu \ll n_\nu^0$ ($n_\nu \gg n_\nu^0$) the value of $\Delta\tilde{m}^2$ tends to the asymptotic value of Δm^2 ($\Delta m_0^2 - \delta$). The choice of n_ν^0 and η are based in some considerations about the relative weight of MaVaN and the MSW mechanism.

In Fig. 1 we plot the effective mass difference, $\Delta\tilde{m}^2$, for some values of n_ν^0 and η . For the choice of the neutrino luminosity $L \sim 10^{51}$ erg s $^{-1}$ and neutrino average energy $\langle E_{\nu_x} \rangle \approx 16$ MeV, we have that for almost any value above $n_\nu^0 > 10^{28}$ cm $^{-3}$ and $\eta < 1$ the effective mass difference $\Delta\tilde{m}^2$ reaches the vacuum mass difference Δm_0^2 , inside the supernova. For comparison, the model presented in [15] is very well reproduced by choosing $\delta = 10$ eV 2 , $\eta = 1$, and $n_\nu^0 = 34500$ cm $^{-3}$, but for these parameters we have no overlap for MaVaN and MSW effects.

The MaVaN mechanism with MSW effects will be effectively given by changing $\Delta m_0^2 \rightarrow \Delta\tilde{m}^2$ in Eqs. (1)–(5). The interplay between the MaVaN effect with MSW effect is very effective when the resonance condition happens for the effective mass difference

$$V(r) = \pm \frac{\Delta\tilde{m}^2(r)}{2E} \cos 2\theta, \quad (11)$$

with the $+$ ($-$) sign attributed to neutrinos (antineutrinos). In the MaVaN mechanism, due the $n_\nu \sim r^{-2}$ asymptotic behavior, we can have the $\Delta\tilde{m}^2(r)$ changing the sign inside the supernova, from positive to negative values, including the point where $\Delta\tilde{m}^2(r) \rightarrow 0$ as shown in the bottom part of Fig. 1. In this region nonadiabatic matter effects can happen.

Figure 2 shows the electronic potential (V_e , solid line) and the right side of Eq. (11) for antineutrinos, with the minus sign, for $\Delta m_0^2 = 1$ eV 2 (dashed line) and $\Delta m^2 = 1.4$ eV 2 (dotted line), for a value of $\tan^2\theta = 2.5 \times 10^{-5}$ and $\delta = 2$ eV 2 with an average neutrino energy $\langle E_\nu \rangle = 15$ MeV. We have chosen the δ parameter inside the range

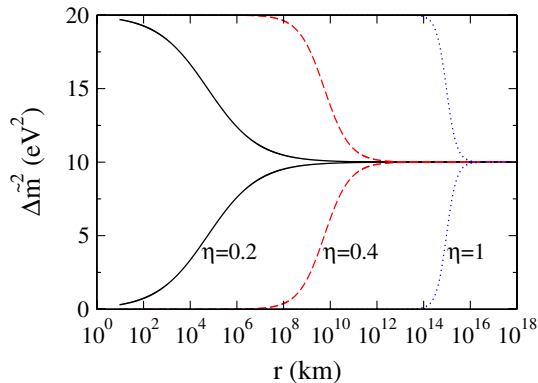


FIG. 1 (color online). The evolution of $\Delta\tilde{m}^2$ from Eq. (9) is shown for $\Delta m_0^2 = 10$ eV 2 , $\delta = \pm 10$ eV 2 and $n_\nu^0 = 10^{25}$, 10^{15} , and 34500 cm $^{-3}$ for the solid, dashed, and dotted lines, respectively. The values for the parameter are shown in the plot. Upper curves for negative and lower curves are for positive δ .

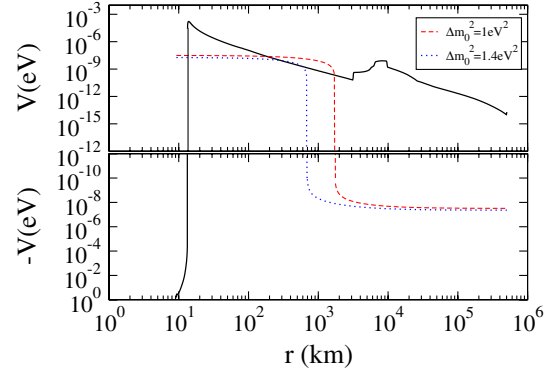


FIG. 2 (color online). The solid curve represents the electronic potential (V_e), calculated from Eq. (6). Dotted (dashed) curve is the right side of Eq. (11) for antineutrinos, for $\Delta m_0^2 = 1.4(1)$ eV 2 , with $\delta = 2$ eV 2 and $(n, n_\nu^0) = (0.5, 1 \times 10^{28}$ cm $^{-3}$) for $\tan^2\theta = 2.5 \times 10^{-5}$ and $\langle E_\nu \rangle = 15$ MeV.

$\delta = 1$ – 20 eV 2 , so that the effect of new physics does not disturb the adiabatic effects that happen for $\Delta m_0^2 \geq 100$ eV 2 , as discussed before. In this way the new MaVaN effects can be analyzed more independently, avoiding a disturbance in the standard adiabatic effects in the inner region of supernova for large values of Δm_0^2 , around a radial distance of 10 km. In the MaVaN framework, from Fig. 2, it is possible to see the appearance of new resonance points. Now we have fixed the range for the parameters δ and n_ν^0 , and we can begin to study the MaVaN phenomenology.

IV. RESULTS AND DISCUSSION

It is possible to constrain the oscillation parameters, such as the mixing angle and the squared mass difference, from the SN1987A data [42–44] in a number of ways. One of them comes from the spectrum of the observed events, probably dominated by $\bar{\nu}_e$. From the observed energy spectrum of SN1987A, the analysis from Kamiokande indicate that the temperature of $\bar{\nu}_e$ is lower than the expectation [45]. The second constraint comes from the expanding envelope driven by thermal neutrino wind of the supernova which is a possible site of heavy nuclei formation beyond iron (r-process nucleosynthesis). Since the ν_e and $\bar{\nu}_e$ conversion into a sterile state (or even into an active state) happens in different rates, the fraction of neutrons to protons, determined by $\bar{\nu}_e + p \rightarrow e^+ + n$ and $\nu_e + n \rightarrow e^- + p$, is modified by the oscillation mechanism in a radial distance from the center of the star of about a hundred kilometers. Related to this constraint, a very simple bound is $Y_e < 0.5$, which can be extracted from Eq. (7) simply considering a very neutron-rich environment [26,27]. In [26] it is shown that Y_e has a dependence on the neutrino oscillations probabilities given by

$$Y_e \sim \frac{1}{1 + P_{\bar{\nu}_e \nu_e} \langle E_{\bar{\nu}_e} \rangle / P_{\nu_e \nu_e} \langle E_{\nu_e} \rangle}, \quad (12)$$

where $P_{\bar{\nu}}$ and P_{ν} are, respectively, the survival probabilities of antineutrinos and neutrinos. From this expression, we clearly see that it is possible to constrain the oscillation parameters from $Y_e < 0.5$. In [45], it is also discussed another constraint based on the fact that the first or the second event of Kamiokande could be related with ν_e . Recent analysis of SN1987A data can constrain the $\bar{\nu}_e$ supernova emission model [46].

We divide this section into two parts. The first one concerns the analysis of the oscillation of active electronic (anti)neutrinos to sterile (anti)neutrinos. In the second section we discuss the possible limits imposed by r-process nucleosynthesis in the oscillation parameter space. In these subsections we will compare the case of MaVaN scenario, presented in Sec. III, with the case of standard oscillations.

A. (Anti)neutrinos

Here we calculate the survival probability $P_{\bar{\nu}}$ for the $\bar{\nu}_e \rightarrow \bar{\nu}_s$ channel of oscillation. Based on the data from SN1987A and neutrino oscillation only in two families, several articles, such as [26], discuss that the survival probability cannot be less than 0.5, for a $\bar{\nu}_e \rightarrow \bar{\nu}_s$ conversion. In this way, it is possible to find regions of exclusion in the oscillation parameter space ($\Delta m_0^2, \tan^2\theta$).

We will find probabilities in the context of the MaVaN parameterization, given by Eq. (9), where we have chosen the sets for (η, n_ν^0) as given in Table I.

In Fig. 3 we show the isocurves of average probability in the oscillation parameter space ($\Delta m_0^2, \tan^2\theta$) with MaVaN] in this figure we use the first line of the Case 1 in Table I: $(\eta, n_\nu^0) = (0.5, 1 \times 10^{28} \text{ cm}^{-3})$ and $\delta = +20 \text{ eV}^2$] and without MaVaN. The thicker curves in Fig. 3 are for the situation without MaVaN and thinner ones represent the situation with MaVaN. In the standard scenario without MaVaN, for lower masses $\Delta m_0^2 \ll 10 \text{ eV}^2$ and $\tan^2\theta \ll 10^{-1}$, the survival probability is greater than 0.7 and then in agreement with SN1987A data. When we include MaVaN, with the parameters in the Case 1 of Table I, we have the presence of new area in the region of $\tan^2\theta \approx 10^{-6}-10^6$ and $\Delta m_0^2 \approx 1-10 \text{ eV}^2$ with survival probabilities smaller than 0.5 in direct contradiction with SN1987A data. Then in this case we can exclude oscillation parameter regions that cannot be tested in the standard scenario. The isocontours are different depending on whether the resonance condition is being fulfilled or not.

To explain the appearance of these new regions we should resort to Fig. 1. The effective mass difference in

TABLE I. Three sets (η, n_ν^0, δ) of our MaVaN model.

Case	η	n_ν^0	δ	Figure
Case 1	0.5	1.0×10^{28}	$+20 \text{ eV}^2$	Figure 3
Case 1	0.5	1.0×10^{28}	-20 eV^2	Figure 4
Case 2	0.8	1.5×10^{30}	$+20 \text{ eV}^2$	Figure 5

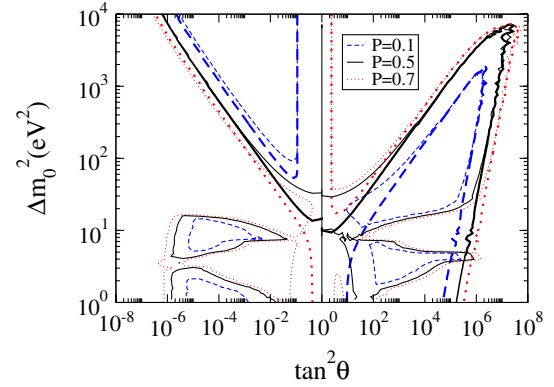


FIG. 3 (color online). Isocurves of survival probability (P). The dashed represents $P = 0.1$, the solid one $P = 0.5$, and the dotted curve $P = 0.7$. The curve evolution set $(\eta, n_\nu^0) = (0.5, 1 \times 10^{28} \text{ cm}^{-3})$ (Case 1) for $\delta = 20 \text{ eV}^2$. In this figure, the thicker curves represent the Case without MaVaN ($\delta = 0$).

MaVaN mechanism, $\Delta\tilde{m}^2(r)$, can change sign inside the supernova, leading to new resonances that were not present before. In standard oscillation scenario without MaVaN, the right side of Eq. (5) is always negative and the resonance condition is never fulfilled. But in the MaVaN mechanism, the effective mass difference $\Delta\tilde{m}^2$ changes sign inside the supernova, as shown in Fig. 2, and now it is possible to fulfill the condition of Eq. (11).

To test the robustness of our analysis, we choose a negative value for δ parameter ($\delta = -20 \text{ eV}^2$) as described in the second line of the Case 1 in Table I: $(\eta, n_\nu^0) = (0.5, 1 \times 10^{28} \text{ cm}^{-3})$. The results are shown in Fig. 4 by the isocontours with MaVaN (thinner curves) and without MaVaN scenario (thicker curves). Although there are changes of the isocontour curves of survival average probability with MaVaN compared with the usual scenario without MaVaN, they are smaller than the case of positive δ . Then we can conclude that only a positive δ will change

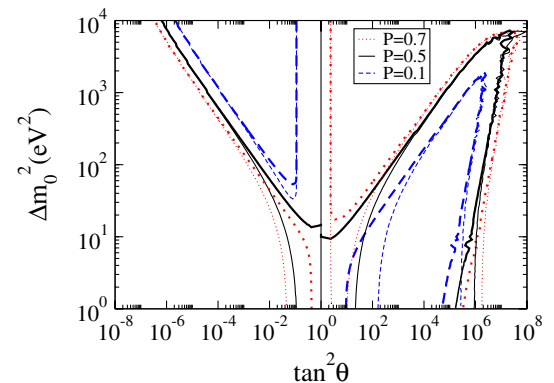


FIG. 4 (color online). Isocurves of survival probability (P). The dashed represents $P = 0.1$, the solid one $P = 0.5$ and the dotted curve $P = 0.7$. The curve evolution set $(\eta, n_\nu^0) = (0.5, 1 \times 10^{28} \text{ cm}^{-3})$ (Case 1) for $\delta = -20 \text{ eV}^2$. In this figure, the thicker curves represent the Case without MaVaN ($\delta = 0$).

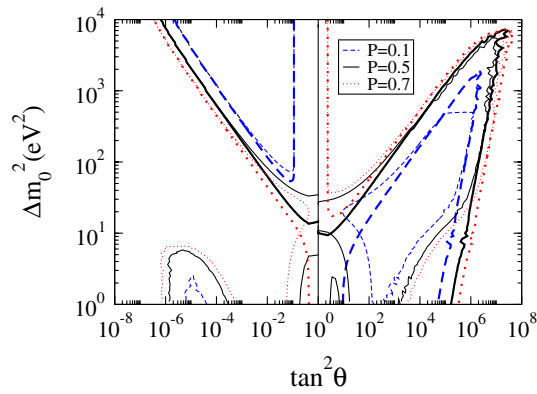


FIG. 5 (color online). Isocurves of survival probability (P). The dashed represents $P = 0.1$, the solid one $P = 0.5$, and the dotted curve $P = 0.7$. The curve evolution set $(\eta, n_\nu^0) = (0.8, 1.5 \times 10^{30} \text{ cm}^{-3})$ (Case 2) for $\delta = 20 \text{ eV}^2$. In this figure, the thicker curves represent the Case without MaVaN ($\delta = 0$).

significantly the antineutrino survival probability and then could be ruled out by SN1987A data. For smaller values of δ , the MaVaN mechanism is even less important, and there is a very small modification in the isocontours of survival average probability if we compare with the standard scenario.

Another test is obtained by changing the parameter n_ν^0 using the Case 2 in Table I as shown in Fig. 5, where $(\eta, n_\nu^0) = (0.8, 1.5 \times 10^{30} \text{ cm}^{-3})$ and $\delta = +20 \text{ eV}^2$. For this choice with higher values of n_ν^0 or η , the values of the isocontour curves of the average probability in the bottom part of Fig. 5 shrink to smaller values of vacuum mass differences and mixing angles if compared to the situation shown in Fig. 3. For even higher values of (η, n_ν^0) , new isocontour regions are even smaller (negligible) and closer to the $\delta = 0$ solution because the condition of Eq. (11) is reached only in the inner parts of supernova, where nonadiabatic effects are dominant and then the survival probability is near the maximum.

From these tests, we conclude that in the MaVaN mechanism is possible to change the isocontours of survival probability as shown in Figs. 3 and 5 for the optimal values of MaVaN parameters as described in Case 1 of Table I. If we remove some of our assumptions, the coexistence of MaVaN and MSW effects and the adiabaticity of inner resonance, then we can have a different range for MaVaN parameters; hence the allowed region for the oscillation also will change.

B. r-process

The production of heavy nuclei in supernova is still an open problem. The region between the protoneutron star and the escaping shock wave a few seconds after the bounce may be a good site for this process, with high entropy and an excess number of neutrons. From β

reactions, $\bar{\nu}_e p \rightarrow ne^+$ and $\nu_e n \rightarrow pe^-$, a modification in the n/p fraction could happen if one considers neutrino oscillation [27,47]. We will analyze what happens with this condition in the context of our MaVaN parameterization and for $\bar{\nu}_e \rightarrow \bar{\nu}_s$ and $\nu_e \rightarrow \nu_s$. We limit our analysis of neutrino flavor conversion to about $r < 50 \text{ km}$, i. e., a region where there is not any shock wave and has a higher influence on antineutrinos. This is approximately the region where the r-process nucleosynthesis happens. For a review of this subject see [48].

From Fig. 2 one can observe that resonances can occur inside the nucleosynthesis region ($r \approx 50 \text{ km}$). Nevertheless such resonances are extremely nonadiabatic when small values of Δm_0^2 are taken into consideration. Therefore, they will not affect the relevant nucleosynthesis. Furthermore, if one considers large values of Δm_0^2 , no resonance happens inside the relevant nucleosynthesis region. In conclusion, our parameter choice implies that one does not expect any significant change in nucleosynthesis processes.

The evolution of $\Delta \tilde{m}^2$ represented by the dotted line in Fig. 1 and its implication in the r-process nucleosynthesis and oscillation probabilities were discussed in [49].

V. CONCLUSIONS AND OUTLOOK

In this paper we proposed a new phenomenological parameterization for the variation of the relevant neutrino oscillation parameters generally presented in MaVaN models, characterized by the parameters (η, n_ν^0) and δ . We analyzed the neutrino and antineutrino survival probabilities for the channels $\bar{\nu}_e \rightarrow \bar{\nu}_s$ and $\nu_e \rightarrow \nu_s$ in the two-flavor context with and without MaVaN. We studied the constraints on the mixing angle and vacuum mass difference coming from r-process and the SN1987A data.

Assuming that MaVaN effects and MSW effects are equally important and the conditions about adiabaticity of resonances are maintained, we imposed a range for MaVaN parameters (η, n_ν^0) that satisfied $n_\nu^0 > 10^{28} \text{ cm}^{-3}$ and $\eta < 1$. In this range we found that the antineutrino survival probability behavior change, allowing smaller values of survival probability— $P \sim 0.5$ —for very small mixing angles, 10^{-6} – 10^{-2} and small vacuum mass difference, $\Delta m_0^2 = 1$ – 20 eV^2 that are in contradiction with SN1987A data. Then, if the MaVaN mechanism is effective with the MaVaN parameters in the range that we considered, we can rule out regions of parameter space that were allowed in standard scenario, without MaVaN's effects.

We also studied the r-process nucleosynthesis condition $Y_e < 0.5$ which is always fulfilled, independent of the oscillation parameters. Then this procedure failed to produce any constraint.

For the next galactic supernova we expect a much larger amount of events coming from $\bar{\nu}_e$ and ν_e elastic scattering. Then we consider that a good understanding of what happens to electronic neutrinos and antineutrinos inside the supernova, in the context of (anti)neutrino oscillations, is crucial to understand the signal that will be detected. Any discrepancy between experimental results and theoretical predictions will point to new physics. In special we presented that MaVaN mechanism can distort the neutrino and antineutrino probabilities and be a source of this discrepancy. Needless to say that, for antineutrinos, the sample data will be larger and with higher statistics the probability to find new phenomena will increase.

ACKNOWLEDGMENTS

The authors are thankful for the ICTP, FAPESP, CNPq and CAPES and Fulbright commission for financial support. We are also thankful for the useful comments and suggestions made by C. A. Moura. We are very grateful for the supernova profile supplied by the Dr. H.T. Janka. F. R.-T. is also thankful for the hospitality of Laboratori Nazionali del Gran Sasso (LNGS) where this work was partially developed. O.L.G. P. thanks the C.N. Yang Institute at Stony Brook University for the hospitality where this work was partially developed.

-
- [1] A. G. Riess *et al.* (Supernova Search Team Collaboration), *Astrophys. J.* **607**, 665 (2004).
- [2] P. Astier *et al.* (The SNLS Collaboration), *Astron. Astrophys.* **447**, 31 (2006).
- [3] D. N. Spergel *et al.* (WMAP Collaboration), *Astrophys. J. Suppl. Ser.* **148**, 175 (2003); D. N. Spergel *et al.* (WMAP Collaboration), *Astrophys. J. Suppl. Ser.* **170**, 377 (2007).
- [4] M. Tegmark *et al.* (SDSS Collaboration), *Phys. Rev. D* **74**, 123507 (2006).
- [5] A. D. Dolgov, arXiv:hep-ph/0405089.
- [6] J. Frieman, M. Turner, and D. Huterer, *Annu. Rev. Astron. Astrophys.* **46**, 385 (2008); E. J. Copeland, M. Sami, and S. Tsujikawa, *Int. J. Mod. Phys. D* **15**, 1753 (2006); P. J. E. Peebles and B. Ratra, *Rev. Mod. Phys.* **75**, 559 (2003); R. R. Caldwell and M. Kamionkowski, *Annu. Rev. Nucl. Part. Sci.* **59**, 397 (2009).
- [7] F. Vissani, G. Pagliaroli, and F. L. Villante, *Nuovo Cimento Soc. Ital. Fis. C* **032**, 353 (2010).
- [8] H. A. Bethe and J. R. Wilson, *Astrophys. J.* **295**, 14 (1985).
- [9] P. Q. Hung, arXiv:hep-ph/0010126.
- [10] R. Fardon, A. E. Nelson, and N. Weiner, *J. Cosmol. Astropart. Phys.* **10** (2004) 005.
- [11] D. B. Kaplan, A. E. Nelson, and N. Weiner, *Phys. Rev. Lett.* **93**, 091801 (2004).
- [12] N. Afshordi, M. Zaldarriaga, and K. Kohri, *Phys. Rev. D* **72**, 065024 (2005).
- [13] O. E. Bjaelde, A. W. Brookfield, C. van de Bruck, S. Hannestad, D. F. Mota, L. Schrempp, and D. Tocchini-Valentini, *J. Cosmol. Astropart. Phys.* **01** (2008) 026.
- [14] V. Barger, P. Huber, and D. Marfatia, *Phys. Rev. Lett.* **95**, 211802 (2005); V. Barger, D. Marfatia, and K. Whisnant, *Phys. Rev. D* **73**, 013005 (2006).
- [15] M. Cirelli, M. C. Gonzalez-Garcia, and C. Pena-Garay, *Nucl. Phys. B* **719**, 219 (2005).
- [16] M. C. Gonzalez-Garcia, P. C. de Holanda, and R. Zukanovich Funchal, *Phys. Rev. D* **73**, 033008 (2006).
- [17] P. H. Gu, X. J. Bi, and X. m. Zhang, *Eur. Phys. J. C* **50**, 655 (2007).
- [18] P. H. Gu, X. J. Bi, B. Feng, B. L. Young, and X. Zhang, *Chinese Phys. C* **32**, 530 (2008).
- [19] T. Schwetz and W. Winter, *Phys. Lett. B* **633**, 557 (2006).
- [20] K. Abe *et al.* (Super-Kamiokande Collaboration), *Phys. Rev. D* **77**, 052001 (2008).
- [21] K. M. Zurek, *J. High Energy Phys.* **10** (2004) 058.
- [22] P. C. de Holanda, *J. Cosmol. Astropart. Phys.* **07** (2009) 024.
- [23] H. Li, B. Feng, J. Q. Xia, and X. Zhang, *Phys. Rev. D* **73**, 103503 (2006).
- [24] E. Komatsu *et al.*, *Astrophys. J. Suppl. Ser.* **192**, 18 (2011); Also for more information see website <http://map.gsfc.nasa.gov/news/index.html>.
- [25] A. Kusenko, *AIP Conf. Proc.* **917**, 58 (2007).
- [26] H. Nunokawa, J. T. Peltoniemi, A. Rossi, and J. W. F. Valle, *Phys. Rev. D* **56**, 1704 (1997).
- [27] J. Fetter, G. C. McLaughlin, A. B. Balantekin, and G. M. Fuller, *Astropart. Phys.* **18**, 433 (2003); G. C. McLaughlin, J. M. Fetter, A. B. Balantekin, and G. M. Fuller, *Phys. Rev. C* **59**, 2873 (1999).
- [28] R. D. Peccei, *Phys. Rev. D* **71**, 023527 (2005).
- [29] H. Minakata, H. Nunokawa, R. Tomas, and J. W. F. Valle, *J. Cosmol. Astropart. Phys.* **12** (2008) 006.
- [30] M. Cirelli, G. Marandella, A. Strumia, and F. Vissani, *Nucl. Phys. B* **708**, 215 (2005).
- [31] L. Wolfenstein, *Phys. Rev. D* **17**, 2369 (1978); S. P. Mikheev and A. Y. Smirnov, *Yad. Fiz.* **42**, 1441 (1985) [*Sov. J. Nucl. Phys.* **42**, 913 (1985)]; S. P. Mikheev and A. Yu. Smirnov, *Nuovo Cimento Soc. Ital. Fis. C* **9**, 17 (1986).
- [32] K. Kainulainen, J. Maalampi, and J. T. Peltoniemi, *Nucl. Phys. B* **358**, 435 (1991).
- [33] B. Dasgupta and A. Dighe, *Phys. Rev. D* **77**, 113002 (2008).
- [34] A. Friedland, *Phys. Rev. Lett.* **104**, 191102 (2010).
- [35] H. Duan, G. M. Fuller, J. Carlson, and Y. Z. Qian, *Phys. Rev. Lett.* **97**, 241101 (2006).
- [36] B. Dasgupta, A. Dighe, G. G. Raffelt, and A. Yu. Smirnov, *Phys. Rev. Lett.* **103**, 051105 (2009).
- [37] C. Giunti and C. W. Kim, *Fundamentals of Neutrino Physics and Astrophysics* (Oxford University Press, Oxford, 2007).
- [38] M. T. Keil, G. G. Raffelt, and H. T. Janka, *Astrophys. J.* **590**, 971 (2003).

- [39] T. Totani, K. Sato, H.E. Dalhed, and J.R. Wilson, *Astrophys. J.* **496**, 216 (1998).
- [40] M. Rampp and H.T. Janka, *Astron. Astrophys.* **396**, 361 (2002).
- [41] U. Franca, M. Lattanzi, J. Lesgourgues, and S. Pastor, *Phys. Rev. D* **80**, 083506 (2009).
- [42] K. S. Hirata *et al.* (Kamiokande-II Collaboration), *Phys. Rev. D* **38**, 448 (1988); K. Hirata *et al.* (Kamiokande-II Collaboration), *Phys. Rev. Lett.* **58**, 1490 (1987).
- [43] R. M. Bionta *et al.* (IMB Collaboration), *Phys. Rev. Lett.* **58**, 1494 (1987); C. B. Bratton *et al.* (IMB Collaboration), *Phys. Rev. D* **37**, 3361 (1988).
- [44] E. N. Alekseev, L. N. Alekseeva, V. I. Volchenko, and I. V. Krivosheina (Baksan Collaboration), *Pis'ma Zh. Eksp. Teor. Fiz.* **45**, 461 (1987) [*JETP Lett.* **45**, 589 (1987)]; E. N. Alekseev, L. N. Alekseeva, I. V. Krivosheina, and V. I. Volchenko (Baksan Collaboration), *Phys. Lett. B* **205**, 209 (1988).
- [45] H. Murayama and T. Yanagida, *Phys. Lett. B* **520**, 263 (2001).
- [46] G. Pagliaroli, F. Vissani, M. L. Costantini, and A. Ianni, *Astropart. Phys.* **31**, 163 (2009).
- [47] Y. Z. Qian, G. M. Fuller, G. J. Mathews, R. W. Mayle, J. R. Wilson, and S. E. Woosley, *Phys. Rev. Lett.* **71**, 1965 (1993).
- [48] M. Arnould, S. Goriely, and K. Takahashi, *Phys. Rep.* **450**, 97 (2007).
- [49] F. Rossi-Torres, M. M. Guzzo, and P. C. de Holanda, *J. Phys. Conf. Ser.* **203**, 012141 (2010).